J. Fluid Mech. (1975), *vol.* 69, *part* 3, *pp.* 417–443
Printed in Great Britain

Waves and turbulence on a beta-plane

By PETER B. RHINES
Woods Hole Oceanographic Institution, Massachusetts 02543

(Received 8 April 1974)

Two-dimensional eddies in a homogeneous fluid at large Reynolds number, if closely packed, are known to evolve towards larger scales. In the presence of a restoring force, the geophysical beta-effect, this cascade produces a field of waves without loss of energy, and the turbulent migration of the dominant scale nearly ceases at a wavenumber $k_\beta = (\beta/2U)^{\frac{1}{2}}$ independent of the initial conditions other than U, the r.m.s. particle speed, and β, the northward gradient of the Coriolis frequency.

The conversion of turbulence into waves yields, in addition, more narrowly peaked wavenumber spectra and less fine-structure in the spatial maps, while smoothly distributing the energy about physical space.

The theory is discussed, using known integral constraints and similarity solutions, model equations, weak-interaction wave theory (which provides the terminus for the cascade) and other linearized instability theory. Computer experiments with both finite-difference and spectral codes are reported. The central quantity is the cascade rate, defined as

$$T = 2\int_0^\infty kF(k)\,dk/U^3\langle k\rangle,$$

where F is the nonlinear transfer spectrum and $\langle k\rangle$ the mean wavenumber of the energy spectrum. (In unforced inviscid flow T is simply $U^{-1}d\langle k\rangle^{-1}/dt$, or the rate at which the dominant scale expands in time t.) T is shown to have a mean value of $3{\cdot}0\times10^{-2}$ for pure two-dimensional turbulence, but this decreases by a factor of five at the transition to wave motion. We infer from weak-interaction theory even smaller values for $k \ll k_\beta$.

After passing through a state of propagating waves, the homogeneous cascade tends towards a flow of alternating zonal jets which, we suggest, are almost perfectly steady. When the energy is intermittent in space, however, model equations show that the cascade is halted simply by the spreading of energy about space, and then the end state of a zonal flow is probably not achieved.

The geophysical application is that the cascade of pure turbulence to large scales is defeated by wave propagation, helping to explain why the energy-containing eddies in the ocean and atmosphere, though significantly nonlinear, fail to reach the size of their respective domains, and are much smaller. For typical ocean flows, $k_\beta^{-1} = 70\,\text{km}$, while for the atmosphere, $k_\beta^{-1} = 1000\,\text{km}$. In addition the cascade generates, by itself, zonal flow (or more generally, flow along geostrophic contours).

1. Introduction

Casual scale analysis of atmospheric and oceanic velocity fields shows nonlinearity to be significant on the energy-containing scale. Realizing this, theoreticians, especially in meteorology, have studied two-dimensional idealizations of a turbulent fluid, omitting for simplicity the mean flow, baroclinity, rotation and orography. The most striking property of two-dimensional turbulence, its inability to dissipate energy at large Reynolds number, had already been realized by Taylor in 1917. Somewhat later it was seen that, if only the energy is spread about a wavenumber space by the nonlinearity, it must move predominantly to large scales. Meanwhile, linearized theories for the ocean and atmosphere were developed which neglected these effects, but included others: wave propagation on a rotating earth, or growth of instabilities on a smooth zonal flow, for example.

Here we want to find how such extremes fare in a combined case, perhaps the simplest model to contain both turbulence and wave propagation. The governing equation for the stream function ψ is

$$D(\nabla^2\psi)/Dt + \beta\psi_x = \nu\nabla^4\psi - R\nabla^2\psi, \tag{1.1}$$

where

$$D/Dt \equiv \partial/\partial t + J(\psi, \ ),$$

$$R = (\nu f/H^2)^{\frac{1}{2}}, \quad f = 2\Omega\sin(\text{latitude})$$

under the usual β-plane approximation (or assuming a physically realizable, slightly sloping, bottom with uniform rotation). Ox and Oy are axes directed east and north, respectively, ν is the kinematic viscosity, Ω the earth's rotation rate, β the mean value of the northward gradient of the Coriolis frequency f, R the bottom drag and the velocity $\mathbf{u} = \hat{\mathbf{j}} \wedge \nabla\psi$, $\hat{\mathbf{j}}$ being an upward unit vector. Preliminary results were reported at the La Jolla IUCRM Symposium, June 1972 (see Rhines 1973).

2. Theory

Two-dimensional turbulence alone

First we describe the extremes. With $\beta = 0$, the dynamics are those of freely migrating source-free turbulence. The subjugation of viscous dissipation at large Reynolds number implies that time dependence, boundary constraints and other force fields will be especially important.

The result of the theory most important here is that the spectral evolution of the energy-containing eddies is predictable under weak assumptions, and independent of detailed inertial-range arguments. The *sense* of the initial evolution (Batchelor 1953, p. 187) is found from the conservation laws for energy and squared vorticity,

$$\frac{\partial}{\partial t}\int_0^\infty E\,dk = -2\nu\int_0^\infty k^2 E\,dk - 2R\int_0^\infty E\,dk, \tag{2.1}$$

$$\frac{\partial}{\partial t}\int_0^\infty k^2 E\,dk = -2\nu\int_0^\infty k^4 E\,dk - 2R\int_0^\infty k^2 E\,dk, \tag{2.2}$$

derived from (1.1), where $E(k)\,dk$ is the contribution to $\frac{1}{2}|\nabla\psi|^2$ from Fourier components with wavenumber $\mathbf{K}$ lying in $k < |\mathbf{K}| < k+dk$, and $k^2E(k)$ is the contribution to $\frac{1}{2}|\nabla^2\psi|^2$ from the same interval. From (2.2), the squared vorticity is non-increasing in time; the right-hand side of (2.1) vanishes as $\nu \to 0, R \to 0$ (Taylor 1917). The right-hand side of (2.2) is the subject of controversy in the inviscid limit, but it is never positive. Hence, if $E(k)$ is specified at $t = 0$ to have a first moment denoted by $\langle k \rangle$, then the postulate that the peak will spread in time, i.e. that

$$\frac{\partial}{\partial t}\int (k-\langle k\rangle)^2 E\,dk > 0,$$

requires [by (2.1) and (2.2)] that

$$\frac{\partial \langle k\rangle}{\partial t} < 0:$$

that the mean wavenumber, with respect to E, decreases. The uneven spreading of energy is required by the 'mass' of $E(k)$ being conserved while its moment of inertia about $k = 0$ is conserved (or decreases). If E is initially very narrow, no significant fraction of the energy (no more than one quarter) can ever reach twice the initial wavenumber. The fluxes of E to small wavenumber, and of k^2E to large wavenumber, correspond in physical space to the formation of ever larger eddies, yet with their vorticity sheared out into ever thinner laminae. The cascade has manifested itself in diverse ways: the clustering of point vortices of like sign (Onsager 1949), which corresponds roughly to interactions among Fourier components of similar wavelength in the continuous case,† and the two-dimensional distortion of small eddies by larger ones, which, if it proceeds in the 'obvious' sense of the distortion of passive dye traces, transfers energy from the small to the large scales (Starr 1968, p. 20). It is interesting that the cascade may be reversed if $\nu \to 0$, $t < \infty$, by changing the sign of the velocity field at any time. But the improbability of a backward cascade occurring is simply the improbability of the thin sheared-out tongues of vorticity in figure 2 (*d*) rewinding themselves.

The *details* of the later spectral evolution are predicted by Batchelor's (1969) similarity theory. If the energy-containing eddies become independent of ν in the inviscid limit, and if they eventually become free of the details of the initial conditions, $E(k, t)$ should depend only on the total energy, the wavenumber and the time. A suitable form is

$$E(k,t) = \tfrac{1}{2}U^3 t f(Ukt) \quad \text{as} \quad \nu \to 0 \quad (t \to \infty), \tag{2.3}$$

where $\frac{1}{2}U^2$ is the (constant) energy density and

$$\int_0^\infty f(\xi)\,d\xi = 1.$$

† Unfortunately, a single point vortex is no longer a steady solution of the equations of motion on a β-plane, and attempts to model turbulence with them will then be misleading. Exact, finite amplitude, westward translating 'vortices' like

$$\psi = J_0(r), \quad r^2 = \tfrac{1}{2}k^2((x-ct)^2+y^2), \quad c = -\beta/k^2,$$

do exist on a β-plane, but they cannot be superposed, nor are they 'isolated'.

The shape f of the spectrum is undetermined; clearly it cannot fit all kinds of initial conditions universally. [For example, only one of Kraichnan's (1967) family of equipartition spectra, $E(k) = k^{-1}$, remains steady according to (2.3).] The flow field implied by (2.3) expands in dominant scale according to

$$d\langle k\rangle^{-1}/dt = TU, \tag{2.4}$$

where

$$T^{-1} = \int_0^\infty \xi f\, d\xi, \quad \text{a constant},$$

$$\langle k\rangle \equiv \int_0^\infty kE\, dk \Big/ \int_0^\infty E\, dk.$$

Values of T somewhat less than unity are expected, in analogy with the 'critically damped' cascade in three-dimensional turbulence, where $U^{-2}dU^2/dt = Ak_1U$; the efficiency A of this cascade ~ 1 if k_1^{-1} is taken to be the integral scale,

$$k_1^{-1} = \frac{3\pi}{4}\frac{\int_0^\infty k^{-1}E\, dk}{\int_0^\infty E\, dk}$$

(Batchelor 1953, p. 103). (The integral scale, proportional to the -1 moment of the spectrum, seems to be greater than a typical rational length scale or even eddy diameter in the flow, and hence the efficiency A will be significantly less than unity when based on such scales.)

What is particularly helpful is that this cascade is so dominated by the spectral peak that we may expect to be able to characterize the flow by *single* scales L, U and $\tau \sim L/U$ (which would not suffice in three dimensions, where the spectra are broader). An experimental test of the similarity theory, and determination of the cascade rate T and its variability, should be a matter of high priority; some partial tests are reported in Batchelor (1969), Lilly (1971) and here in §3. The form (2.3) conserves energy but not total enstrophy. Some comments on this problem, and on inertial subranges, are given in the appendix.

Rossby waves alone

When the nonlinear term in (1.1) is very small, arbitrary initial values of the stream function can be decomposed into plane Rossby waves (plus a geostrophic zonal flow), and the time evolution followed simply. The wavenumber spectrum is invariant in time, if the domain is unbounded. Plane transverse waves $\psi = \exp(i\mathbf{K}.\mathbf{x} - \omega t)$, by the linear inviscid version of (1.1), have the dispersion relation

$$\omega = -\beta \mathbf{K}.\hat{\mathbf{i}}/|\mathbf{K}|^2 \tag{2.5}$$

($\hat{\mathbf{i}}$ and $\hat{\mathbf{j}}$ are eastward and upward unit vectors, respectively), which favours long waves and north–south fluid velocities. The association of large frequencies with large scales is a special feature of these waves, and one that is important in what follows.

The combined case

First consider the constraints analogous to (2.1) and (2.2), taking the inviscid limit. Manipulation of (1.1) leads to an energy equation

$$D(\tfrac{1}{2}|\nabla\psi|^2)/Dt = -\nabla.\mathbf{F},$$

where $\mathbf{F} = -\psi D(\nabla\psi)/Dt + \frac{1}{2}\beta\psi^2\hat{\mathbf{i}}$. The vector $\mathbf{F}$ is not a unique energy flux, but its divergence is unique, and equals $\nabla.$(pressure $\times$ velocity). (This particular $\mathbf{F}$ happens to equal the product of energy density and group velocity in the limit of small amplitude.)

A local conservation law for the enstrophy is found by multiplying (1.1) by $\nabla^2\psi$:

$$D(\tfrac{1}{2}|\nabla^2\psi|^2)/Dt = -\nabla.\mathbf{G},$$

$$\mathbf{G} = -\tfrac{1}{2}\beta(\psi_y^2 - \psi_x^2, -2\psi_x\psi_y) = -\tfrac{1}{2}\beta|\mathbf{u}|^2(\cos 2\theta, \sin 2\theta),$$

where $\mathbf{u} = \hat{\mathbf{j}} \wedge \nabla\psi$ and θ is the angle of $\mathbf{u}$ from east; $\tan\theta = -\psi_x/\psi_y$.† The enstrophy is in part advected, and in part transmitted in a direction $\pi - 2\theta$ by the β-effect. In the limit of small amplitude $\mathbf{G}$ reduces to the product of $\frac{1}{2}|\nabla^2\psi|^2$ and the group velocity.

Integral relations

Taking a region S bounded by a contour $\mathscr{C}$ with outward normal $\mathbf{n}$ and arc length s, (2.5) yields

$$\frac{1}{2}\frac{\partial}{\partial t}\iint_S |\nabla\psi|^2\,dx\,dy = -\oint \mathbf{F}.\mathbf{n}\,ds - \frac{1}{2}\oint |\nabla\psi|^2\mathbf{u}.\mathbf{n}\,ds, \tag{2.6}$$

$$\frac{1}{2}\frac{\partial}{\partial t}\iint_S |\nabla^2\chi|^2\,dx\,dy = -\oint \mathbf{G}.\mathbf{n}\,ds - \frac{1}{2}\oint |\nabla^2\psi|^2\mathbf{u}.\mathbf{n}\,ds. \tag{2.7}$$

In the case of a periodic domain, the right-hand sides both vanish, leaving the usual conservation laws analogous to (2.1) and (2.2). In the oceanically interesting case of rigid lateral boundaries, however, this is no longer true; see §4. For the present we restrict ourselves to a model atmosphere or mid-ocean region with re-entrant geometry in both directions.

Conversion of turbulence to waves

Imagine doing an initial-value experiment in which a closely packed field of eddies with a narrow spectrum peaked at $k = k_0$ is set off and allowed to advect freely. The dividing line between wavelike and turbulent dynamics occurs where the nonlinear and $\beta\psi_x$ term in (1.1) are comparable; that is, where the Rossby wave steepness (the particle excursion divided by a quarter-wavelength, or the root-mean-square fluid velocity U divided by the phase speed c_p corresponding to the dominant scale) is unity. With $c_p = \beta/2k^2$ for an average orientation of the wave crests, this defines the measure of nonlinearity to be $2k_0^2 U/\beta \equiv \epsilon$. In terms

† Exactly analogous relations exist for the physically realizable 'sloping bottom' model of the β-plane.

of spectra, the fluid velocity $\hat{U}(k)$ at a wavenumber k may be defined by integrating over the two octaves surrounding k:

$$\tfrac{1}{2}\hat{U}(k)^2 = \int_{\frac{1}{2}k}^{2k} E(k')\,dk' \approx kE(k)$$

for a smooth distribution $E(k)$. Then the curve corresponding to

$$\hat{U}(k) = c_p(k) = \beta/2k^2,$$

typically, is

$$E_\beta(k) = c_1\beta^2 k^{-5}, \tag{2.8}$$

with c_1 a constant of order unity, and divides turbulence (above) from waves (below). It is very steep because of the rapid increase of wave frequency with scale.

If, then, the initial wavenumber k_0 in this experiment exceeds $k_\beta \equiv \beta/2U$ the dominant eddies will migrate towards large scales, and hence large characteristic times $(kU)^{-1}$ (since energy is nearly invariant). But eventually the motions must evolve into Rossby waves, for the continual increase in both the length scale and advective time scale makes the restraint due to β doubly powerful. If $k_0 \gg k_\beta$, the dominant wavenumber will reach k_β after a time

$$\sim (Tk_0U)^{-1}(1+2+4\ldots k_0/k_\beta) \sim 2^{\frac{3}{2}}/T(\beta U)^{\frac{1}{2}},$$

which is independent of k_0 itself (the estimate TkU for the turbulent interaction rate has been used).

Once the field has reached this scale, wave propagation will begin, and we now make the further suggestion that near k_β the wavenumber cascade will effectively halt. 'Hot spots' of vorticity will begin to radiate away before they are distorted advectively (recall that the cascade hinges on the ability of the shear to elongate vorticity contours into ever thinner sheets). At the same time individual fluid particles will relinquish their random circulations and begin to oscillate about latitude lines.

The hypothesis that the cascade to small wavenumbers will slow up severely as the transition to wave motion occurs seems intuitive, for then weak, selective, spectral interactions replace the indiscriminate cascade of turbulence. But this description conceals the fact that, to the accuracy of scale analysis, second-order wave interactions are just as rapid as turbulence: each occurs in a time $\sim (kU)^{-1}$, even though in the former case many ($\sim \epsilon^{-1}$) wave periods may be required. One suspects, however (and we subsequently demonstrate), that the above estimate represents an interaction of the greatest possible efficiency, which turbulence approaches, yet which weak interactions fall short of, owing to their sensitivity to the relative phases of the Fourier components. Put most simply, wave interactions require wavenumber and frequency resonance, as well as physical coincidence, in order to fulfil the scale analysis of their cascade rate.

The weak-interaction limit: cascade to small wavenumber

Since the nonlinearity sends energy predominantly towards the wave regime, it is of interest to characterize, as generally as possible, the weak interactions that

can occur deep within it. The integral constraints (2.6) and (2.7) apply no matter how weak the nonlinearity, hence a spreading peak of energy must continue to move its centroid to smaller wavenumbers.

Cascade to small frequency

In the turbulent regime the migration to small k is also a migration to small frequency ω, for the two are directly related, roughly with proportionality U. (We are thinking of the frequency that characterizes the Fourier time transform of the velocity over a time interval of several units of $(\langle k\rangle U)^{-1}$.) In the wave regime $\epsilon \ll 1$ there is evidence from weak-interaction theory that the decrease in frequency continues, for it is easily shown that, in a resonant triad, the wave of highest frequency is unstable to growth of small amounts of seed energy in the two remaining numbers. This instability was demonstrated in an apparently general derivation by Hasselmann (1967). Some uncertainty has been expressed about the applicability of the general theory to Rossby waves, however, so we shall verify the result.

The weak-interaction equations for three waves,

$$\psi_i = \mathscr{R} a_i(t) \exp(i\mathbf{K}_i.\mathbf{x} - i\omega_i t), \quad i = 1, 2, 3,$$

are

$$\dot{a}_l = B\frac{k_m^2 - k_n^2}{k_l^2} a_m a_n, \quad l, m, n \text{ cycled}$$

(e.g. Kenyon 1964), where B is twice the area enclosed by the wavenumber triangle, $B = |\mathbf{K}_1 \wedge \mathbf{K}_2|$, $k_i = |\mathbf{K}_i|$, $\Sigma\mathbf{K}_i = \Sigma\omega_i = 0$, and $\omega_i = -\beta\mathbf{K}_i.\hat{\mathbf{i}}/|\mathbf{K}_i|^2$. Frequencies and wavenumbers may take either sign. Following Simmons (1969) we transform to amplitudes whose squares are proportional to energy density, yielding

$$\dot{\hat{a}}_i = C\omega_i \hat{a}_j \hat{a}_k,$$

where $\hat{a}_i = k_i a_i$ (no summation),

$$C = \frac{\beta B}{3k_1 k_2 k_3 \omega_1 \omega_2 \omega_3}[\omega_1(\alpha_2 - \alpha_3) + \omega_2(\alpha_3 - \alpha_1) + \omega_3(\alpha_1 - \alpha_2)],$$

$$\alpha_i = \mathbf{K}_i.\hat{\mathbf{i}}.$$

Conservation of energy follows from the sum of the three equations. The amplitude of each member of the triad changes at a rate directly proportional to its frequency. Take ω_1 to be the largest frequency, then $\omega_1 = -(\omega_2 + \omega_3)$ and ω_2 and ω_3 have the sign opposite to that of ω_1. Now the initial-value problem $\hat{a}_1 = 1$, $\hat{a}_2 = \delta_2 \ll 1$, $\hat{a}_3 = \delta_3 \ll 1$ has solutions $\hat{a}_2, \hat{a}_3 = (\delta_2, \delta_3)\, e^{\lambda t}$ with positive growth rate $\lambda = (\omega_2\omega_3)^{\frac{1}{2}} C|\hat{a}_1|$, yet if $\hat{a}_2 = 1$, say, and $\hat{a}_1 = \delta_1 \ll 1$ and $\hat{a}_3 = \delta_3 \ll 1$, the perturbations are damped, $\lambda^2 = -|\omega_1\omega_3| C^2|\hat{a}_2|^2$, verifying Hasselmann's conclusion. (The amplitudes δ_2 and δ_3 must occur in the ratio $(\omega_2/\omega_3)^{\frac{1}{2}}$ for the unstable case. Arbitrary values of δ_2 and δ_3, specified initially, will excite in addition the damped mode.)

In this particular problem the energy moves predominantly to small frequencies. If the system were closed, with no other wave components admissible, the field would return periodically to its initial configuration, but McEwan (1972)

and Martin, Simmons & Wunsch (1972) have emphasized that the interaction sets are open, allowing a continuous cascade to lower frequencies via an ever widening set of triads. Their experiments, especially the latter, show this preferred sense.

Anisotropy: zonal currents

This movement of energy simultaneously towards small wavenumbers and small frequencies cannot occur with the field remaining isotropic, for the dispersion relation (2.5) would associate small frequencies with *large* wavenumbers if we were to fix the direction of propagation. The fluid must adjust by favouring north–south wavenumbers (east–west currents): the eddies are flattened by the β-effect. Kenyon (1967) found this to occur in particular calculations of the *initial* tendency of a weakly interacting continuous spectrum.

Such production of zonal energy contrasts with the often-cited inability of a precisely zonal current to gain or lose energy from triad interactions with planetary waves (e.g. Longuet-Higgins & Gill 1967; Newell 1970). But a likely end-state of the cascade, in fact, is a steady zonal current, bands of eastward and westward flow alternating with scale somewhat larger than, but of the order of $(2U/\beta)^{\frac{1}{2}}$. This is because, as the anisotropy increases, the north–south velocities become slight perturbations, to which the flow is absolutely stable if $\beta - u_{yy}$ never vanishes ($u = -\psi_y$). Stability in the mean occurs if $\psi_y \gg \psi_x$ and $\beta - U\langle k^4\rangle^{\frac{1}{2}} > 0$. We have shown that the cascade causes $\langle k\rangle^2$ to fall below $\beta/2U$, so that unless $\langle k\rangle^2/\langle k^4\rangle^{\frac{1}{2}}$ is very small (recall the peaked shape of the spectrum) the 'average' flow is indeed stable, and most non-zonal motion will die exponentially away. These remarks apply to homogeneous fields of eddies, but if the energy is intermittent in space, the onset of wave propagation will spread the energy ever more thinly, causing interaction to cease before the zonal state is reached. This will also occur if the eddies are overdamped by friction.

Estimates of the interaction rates: Kenyon's result

It has been conjectured that the wavenumber cascade will proceed much more slowly once the transition to wave motion has occurred. If the nonlinearity were of third order rather than second, resonant interactions would require four waves, and the cascade 'barrier' could be established by scale analysis (one has a feeling for the suddenness of such a linear–nonlinear transition with surface gravity waves). Here, with triad interactions, this cannot be done, and so we look to numerical computations of the interactions like those of Kenyon (1967). One consequence of the Hasselmann formulation for homogeneous fields, of course, is that the solution for the cascade from a given set of waves holds for arbitrary amplitude (so long as it is sufficiently small), the time being rescaled by the average wave steepness. Thus, the weak-interaction theory predicts T to be *independent of* ϵ for $\epsilon \ll 1$.

Kenyon used two model spectra as initial conditions for this tendency calculation. From the first, a narrow-band spectrum centred on $(0, -k)$ with an angular dispersion of 22° and wavelength dispersion of 10%, we estimate $T \approx 4 \times 10^{-3}$. The second model was isotropic, with the same wavelength distribution, and led to a value of T so small that it was not measurable from the published figure. This

is not to say that the resonant interactions were all inefficient, but most of the initial change in the spectrum involved orientation, rather than wavelength. To see this, we estimated a second version of the cascade rate:

$$T' = \int_0^\infty |d\hat{E}(\mathbf{K})/dt|\, d\mathbf{K}/U^3\langle k\rangle,$$

which is sensitive to changes in the *vector* wavenumber spectrum $\hat{E}(\mathbf{K})$. The result is much larger estimates $T' = 4{\cdot}7 \times 10^{-2}$ and $3{\cdot}3 \times 10^{-2}$ for the two respective initial conditions.

Lorenz's and Gill's results

The reason for the smallness of T is thus that the wave interactions send energy to other *directions* more readily than to other wavelengths. The different, yet still analytical approach of Lorenz (1972) and Gill (1974) may be used to reach the same conclusion. A single plane Rossby wave of arbitrary amplitude is found to be unstable to the growth of other Fourier components. In the case $\epsilon \ll 1$, we showed earlier that the energy flux from the primary wave into two growing waves, subscripted 1 and 2, occurs in the ratio ω_1/ω_2. Now the resonance conditions mapped out by Gill contrive to give the longest wave of the triad an especially small frequency, and hence the long wave, which would lead to significant T, is in disfavour. A primary wave (ω_0, k_0) directed due west, for example, has most unstable partners $(\omega_1, k_1) = (0{\cdot}80\omega_0, 1{\cdot}09k_0)$ and $(\omega_2, k_2) = (0{\cdot}20\omega_0, 0{\cdot}54k_0)$, with energy flux into the wave of nearly the same length (k_1) which is four times greater than that into k_2. The cascade rate T calculated from Gill's results for the most unstable perturbations to a basic wavenumber $(-k_0, 0)$ is

$$T = 0{\cdot}012m/(1 - 0{\cdot}025m)^2 \approx 0{\cdot}012m,$$

m being the fraction of the total energy lying in the perturbations. The calculation is strictly valid only for small m, but suggests values $T \approx 3 \times 10^{-3}$–$6 \times 10^{-3}$ for a well-developed instability ($m = 0{\cdot}25$–$0{\cdot}5$). The numerical rates are similar to those found from Kenyon's model despite the vastly differing initial conditions.

The calculation also works for large ϵ, providing the simplest imaginable model of the turbulent cascade with negligible wave propagation. In this case $T \approx 0{\cdot}045m$, nearly four times larger than with $\epsilon \ll 1$, approaching $T = 2{\cdot}4 \times 10^{-2}$ at $m = 0{\cdot}5$. The difference is that the aversion to changes in $|\mathbf{K}|$ does not occur in this case, fully 38 % of the energy going to the wavenumber $0{\cdot}59k_0$ and most of the remainder to $1{\cdot}16k_0$.

Both linear and weakly nonlinear theory suggest cascade rates that are similar to those found in the turbulence experiments, to be described below. There are, however, questions about the theory which deserve study. It is difficult to account for the changing bandwidth of the instability, for example, in proceeding from large to small ϵ. But the qualitative feature, the favouring of energy flux to new directions of $\mathbf{K}$ rather than new magnitudes $|\mathbf{K}|$ when β is strong, and the consequent inhibition of the cascade appear to be reliable.

Inhomogeneity: a model cascade

The above estimates suggest that T should be an increasing function of ϵ. If, in addition, the energy is inhomogeneously distributed, this tendency can even be stronger. Within sparsely distributed patches of energy, surrounded by quiet fluid, turbulent interactions will prevail, but, once waves begin to radiate, the energy will quickly be distributed over a broader area, reducing ϵ, and hence the real-time cascade rate $d\langle k\rangle/dt$. But in addition the number of Fourier components present in the far field may be few, making it less likely that conditions for weak resonance will be satisfied. Viscous damping can accentuate this situation by preventing the far-field 'mix' from becoming rich. The contrast between cascade rates (even *after* rescaling by the local ϵ) in the turbulent and wavelike regions will increase with this kind of intermittency.

Consider a model of a turbulent 'spot' which is surrounded by fluid at rest; classically this would be an entrainment problem. Take the dominant diameter of the energy-containing eddies to be L, the radius of the patch to be R ($\gg L$) and a typical velocity of the eddies within to be U. A plausible set of model equations is

$$\dot{R} = \beta L^2, \quad \dot{L} = TU, \quad UR = U_0 R_0, \tag{2.9}$$

where the dots denote time derivatives and β, T, U_0 and R_0 are constants. The first relation says that the region of motion expands into its surroundings at the group velocity of Rossby waves (ignoring anisotropic effects), the second, that the dominant scale increases at a rate TU, and the third, that the total kinetic energy is conserved.

The implicit solution is

$$R = R_0 \exp\left(\frac{\beta}{3U_0 R_0 T}(L^3 - L_0^3)\right), \quad t - t_0 = (TU_0)^{-1}\int_{L_0}^{L} \frac{R(L')}{R_0}\,dL',$$

where a subscript zero indicates a prescribed initial value. The dependence of R upon L is so severe as to resemble a step function. Initially the eddy scale L increases linearly, without a great change in R, then the patch increases explosively in size, reducing U, and thereafter the change in L is much slower than logarithmic. Time histories of L and R for a particular case are shown in figure 1. The scale L_1 at which linear growth of L ('turbulence') gives way to linear growth of R ('radiation') is $L_1 = (3U_0 R_0/\beta)^{\frac{1}{3}}$.

A termination of the cascade can thus occur through the spreading of energy in space. The two length scales of the evolved waves given by the entirely different closures have a ratio $k_\beta L_1 = 3^{\frac{1}{3}}(\beta R_0^2/U_0)^{\frac{1}{6}}$. $k_\beta L_1$ is nearly unity for geophysical choices of the initial conditions. The same parameter, $\beta R_0^2/U_0$, determines whether a patch of turbulence is effectively unbounded (if large), L tending to k_β^{-1} before radiation to the exterior has an effect, or effectively intermittent (if small or order unity). The model could be criticized for overestimating R in the nonlinear regime and overestimating L in the linear regime, but more accurate expressions would only accentuate the tendency for R to 'explode' and L to equilibrate.

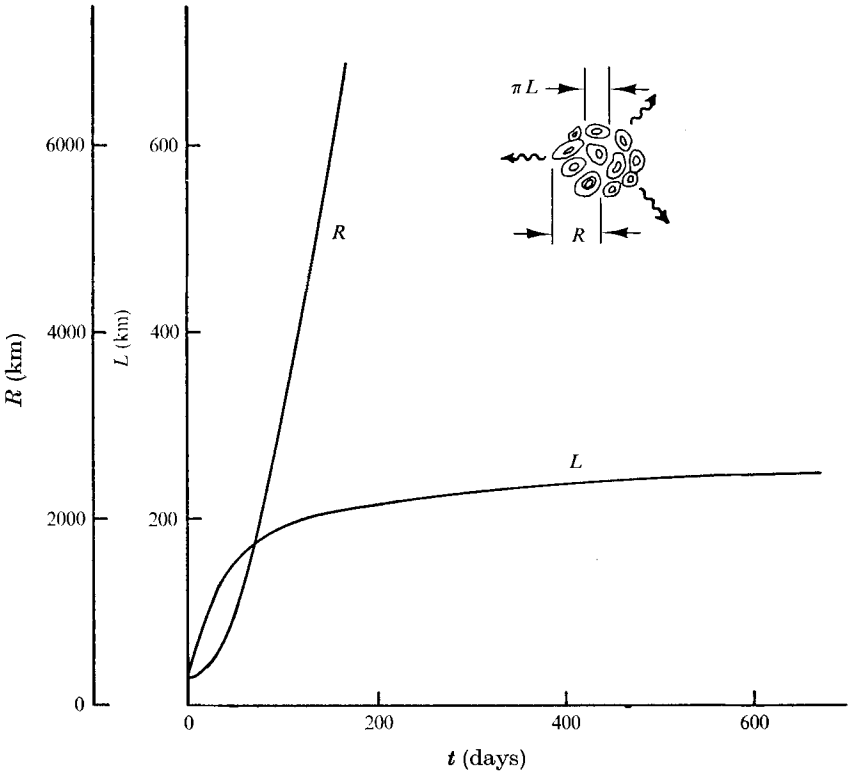

FIGURE 1. Growth with time of the radius R of an *isolated* region of eddies of (changing) length scale L, according to the simple model equations (2.10).

Equilibrium spectrum?

It can be argued that the slowing down of the cascade once the spectrum has crossed the transition will cause a statistically steady spectrum $E \approx E_\beta(k)$ to develop. For this to work, energy must constantly be supplied, and either dissipated at wavenumbers near k_β or allowed to fill out the equilibrium spectrum at ever smaller wavenumbers. The detailed arguments for the development of equilibrium share some of the difficulties of other predicted, steep, geophysical equilibrium spectra, and make the precise power law uncertain. A superficially appealing statement is that in each band of wavenumbers energy in excess of $E_\beta(k)$ will be 'turbulent' with large cascade rate T and will flow to smaller wavenumbers until that band just becomes wavelike, inhibiting further change. This is like the local saturation of wind waves (Phillips 1966), but in reverse. The difficulty is that, with a k^{-5} law, the shear working on eddies of wavenumber k is really dominated by those of smaller wavenumber (lying near the spectral peak), making the local argument suspect. Nevertheless the k^{-3} spectra of two-dimensional turbulence and of wind waves have been useful, if temporary (and often overstressed) ideas. The corresponding dimensional argument, that the spectrum should depend only on β and k itself at large Reynolds number and far from the peak, is unconvincing for the same reason, that the position of the spectral peak is a vital parameter.

The conclusion is that this flow is dominated by the energy-containing eddies and, better even than two-dimensional turbulence, characterized by single dominant scales U, k and $\tau \sim (k_\beta U)^{-1}$. In a steadily forced flow the spectrum should develop a peak at k_β, decreasing rapidly towards larger k.

3. Numerical experiments

To test these ideas, (1.1) was integrated by a CDC 6600-7600 computer. Three different programs, and two different numerical schemes, were used: first, a 64×64 finite-difference model (called FD64 here) with a second-order Arakawa formulation of the nonlinearity and Adams–Bashforth time step. This was essentially the coding used by Lilly (1969 ff.) in his successful studies of two-dimensional turbulence. Subsequently, 128×128 (SP128) and 64×64 (SP64) Fourier-mode Galerkin programs were used, borrowing the coding developed by Orszag (1971) and Fox & Orszag (1972), with centred time differencing and removal of all aliasing effects. Each program was tested with known analytic solutions. Linear Rossby-wave propagation was accurate for wavelengths greater than 6 grid intervals or so (FD64) and nearly perfect in the spectral model (but for errors in time stepping). An advection test was made, similar to Orszag's test with coloured cones, in which a small Gaussian vortex was superimposed upon a disk-like rotation of the fluid (any steady solution may be rotated, with $\beta = 0$). The test seemed severe, but vortices of diameter four times the cut-off wavelength (spectral model) moved several diameters before distorting noticeably. The spectral code was able to produce thinly sheared-out vorticity contours (figure 2*a*) rather better than the finite-difference model. Seven turbulence experiments are described here, representing perhaps two-thirds of the number carried out. The remainder were rejected only because of obvious numerical inaccuracy or outright instability. Table 1 gives a summary of the runs. The intention is not to make exhaustive comparison of different numerical schemes: see Orszag (1971) and Herring *et al.* (1974) for such information.

Turbulence alone

Experiments similar to Lilly's (1971) work were repeated with each of the programs (runs 1, 2 and 3) as controls, and because experimental values for T with pure turbulence are of interest in themselves. Values of the stream function were initially set by choosing randomly from the population of Fourier components with scalar wavenumber 7, 8 or 9 (FD64 and SP64) or 11–14 (SP128, figure 2*b*); the wavenumber 1 is periodic in the width of the square box, and an integer wavenumber N refers to all vector wavenumbers falling in a unit annular band of mean radius N. Subsequently the flow was allowed to migrate freely, without forcing, with weak damping and periodic boundary conditions.

A detailed realization of Batchelor's solution for the free cascade is an important goal, but here we can test only the gross behaviour of (2.4). The evolution of the dominant eddies is of more interest to the present problem than the *indirect* measures of the cascade, the dissipation of enstrophy and energy, examined by Lilly (1971). (Recall that Batchelor's (1969) result predicts the

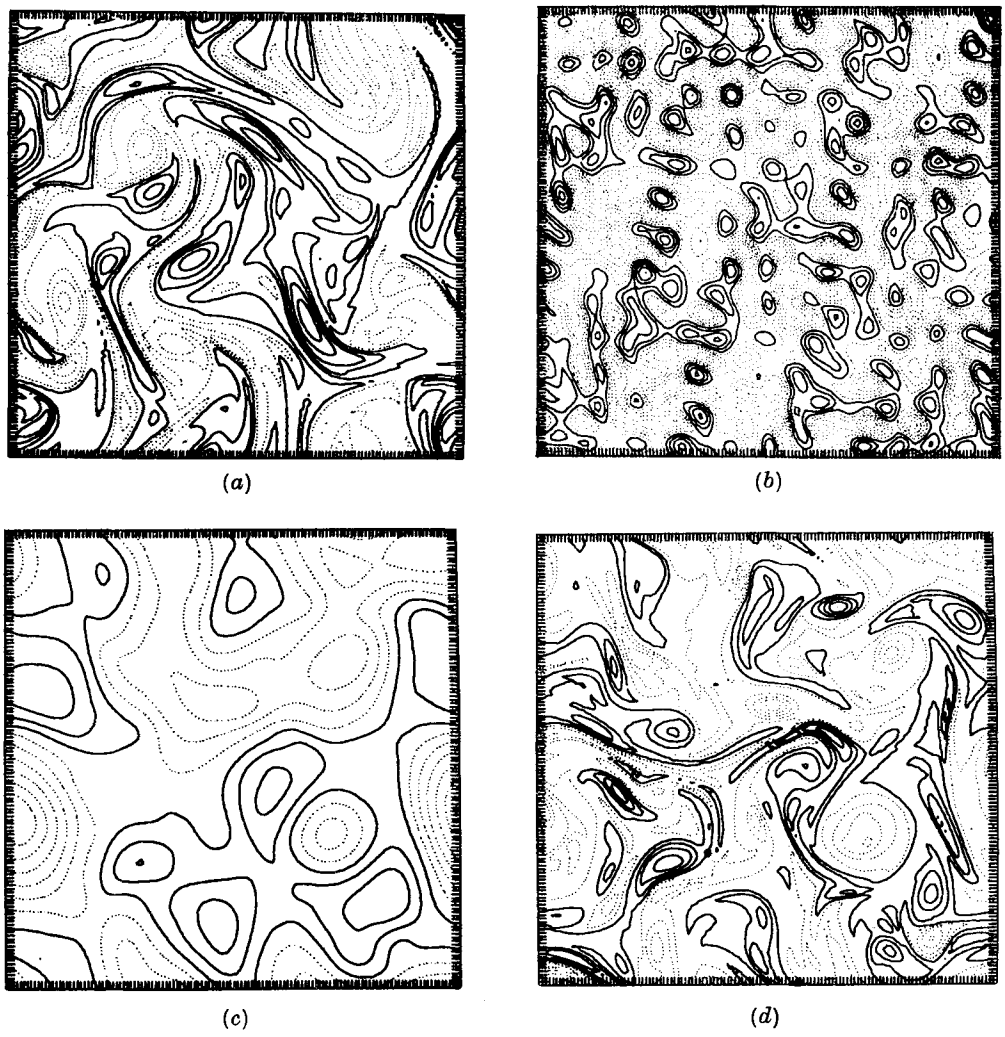

FIGURE 2. (*a*) Vorticity contours for a typical pure-turbulence run, $\beta = 0$, using Fox & Orszag's spectral code. ——, positive; ------, negative. (*b*) Streamline field near the beginning of the free-evolution experiment (21st time step), $\beta = 0$, run 2. Contour interval = 0·038. See table 1 for details. (*c*) Streamlines at $t = 5{\cdot}8$ (725th time step), run 2. Contour interval = 0·1. (*d*) Vorticity contours at $t = 5{\cdot}8$, run 2. Contour interval = 1·3.

enstrophy flux at the upper end of validity of the similarity solution; whether or not this should be equated to the dissipation of enstrophy in these transient flows is unclear. In addition the enstrophy dissipation, $\propto k^4E$, is notoriously difficult to simulate.)

The flow in figure 2 (*b*) (with $\beta = 0$) cascaded in the usual fashion to large scales. Figures 2 (*c*) and (*d*), showing the stream function and vorticity at time $t = 5{\cdot}8$, indicate the irreversible distortion responsible for the enstrophy moving to large wavenumbers. By following the development of the vorticity filaments, one learns to assess the goodness of the simulation; at excessive Reynolds numbers

Run	Model	β	ν	t	R_e	$\langle k\rangle$	ϵ	T_{obs}	T_ν	N	Breadth	c_x	$\beta/\langle k\rangle^2$
1	FD64	0	0·002	0	144	7·76	∞	—	—	—	—	—	—
				1·13	155	6·25	—	—	$<0{\cdot}010$	—	—	—	—
				2·58	218	4·00	—	0·033	0·017	2·9	0·28	—	—
				3·94	331	2·48	—	0·065	$<0{\cdot}027$	3·0	0·55	—	—
				5·07	364	2·17	—	0·030	0·011	3·3	0·79	—	—
2	SP128	0	0·0015	0	72	13·4	—	—	—	—	0·072	—	—
				0·4	79	11·1	—	0·044	0·008	—	0·28	—	—
				2·4	127	5·4	—	0·049	0·013	4·3	0·27	—	—
				5·2	179	3·5	—	—	—	4·3	0·39	—	—
				6·2	190	3·2	—	0·029	0·011	4·4	0·33	—	—
3	SP64	0	0·004	0	31	10·4	—	—	—	—	—	—	—
				2·0	34	5·3	—	—	0·041	5·3	—	—	—
				3·0	40	4·1	—	0·079	0·036	4·5	0·27	—	—
				4·0	41	3·5	—	0·064	—	5·2	—	—	—
				6·0	47	2·8	—	0·069	0·038	4·7	0·28	—	—
				7·0	49	2·6	—	0·059	—	4·5	—	—	—
4	FD64	21	0·004	0	74	7·5	11·6	—	—	—	—	—	—
				0·8	63	7·3	9·1	—	—	—	—	—	—
				1·5	56	6·7	6·2	—	0·0088	5·5	—	0·63	0·47
				2·5	57	5·3	3·2	0·030	0·021	4·2	0·12	0·96	0·76
				4·0	59	4·2	1·7	0·028	0·016	4·6	0·16	—	—
				5·5	59	3·8	1·2	0·021	0·0093	5·0	0·10	1·4	1·2
				7·1	58	3·5	0·94	0·015	—	5·3	—	2·0	—
5	SP128	3·25	0·0015	0	Same as run 2		159	Same as run 2				—	0·02
				3·0			14·8					0·2	0·13
				5·0			6·9					0·6	0·27
				6·2			5·6					—	—
6	SP128	17·3	0·0005	0	101	7·9	2·9	—	0·0009	—	0·025	0·19	0·28
				1·5	101	7·6	2·5	0·019	0·0028	6·1	0·064	0·36	0·36
				3·9	107	6·7	1·9	0·020	0·0054	5·3	0·12	—	—
				4·2	107	6·6	1·8	—	—	5·3	—	0·38	0·40
7	SP64	52	0·004	0	31	10·4	5·2	—	—	—	—	—	—
				1	26	8·5	2·5	—	—	—	—	0·60	0·72
				2	24	7·2	1·4	0·037	0·030	6·7	—	—	—
				3	21	6·4	0·84	0·039	0·029	7·0	0·13	—	—
				4	20	5·7	0·57	0·035	0·028	7·0	—	1·45	1·61
				5	19	5·2	0·42	0·036	0·030	7·0	0·12	—	—
				7	17	4·7	0·27	0·031	0·029	7·0	0·08	2·36	2·36

TABLE 1. The computer experiments. FD refers to finite-difference model, SP to spectral model, 64 and 128 to the (degrees of freedom)$^{\frac{1}{2}}$, ν is viscosity, t is the time, R_e the Reynolds number $U/\langle k\rangle\nu$, based on the r.m.s. velocity U and the centroid $\langle k\rangle$ of the wavenumber spectrum. ϵ is the wave steepness $2U\langle k\rangle^3/\beta$, T_{obs} is the observed cascade rate $U(t)^{-1}d\langle k\rangle/dt$, T_ν is the viscous correction (figure 4 plots $T_{obs}-T_\nu$), N is the power in the approximate power law of the spectral tail $E\propto k^{-N}$ (omitting the highest octave (64^2) or two octaves (128^2)). B is the 'breadth' of the spectrum, c_x is the observed westward phase speed, and $\beta/\langle k\rangle^2$ is the corresponding linear phase speed based on the centroid wavenumber.

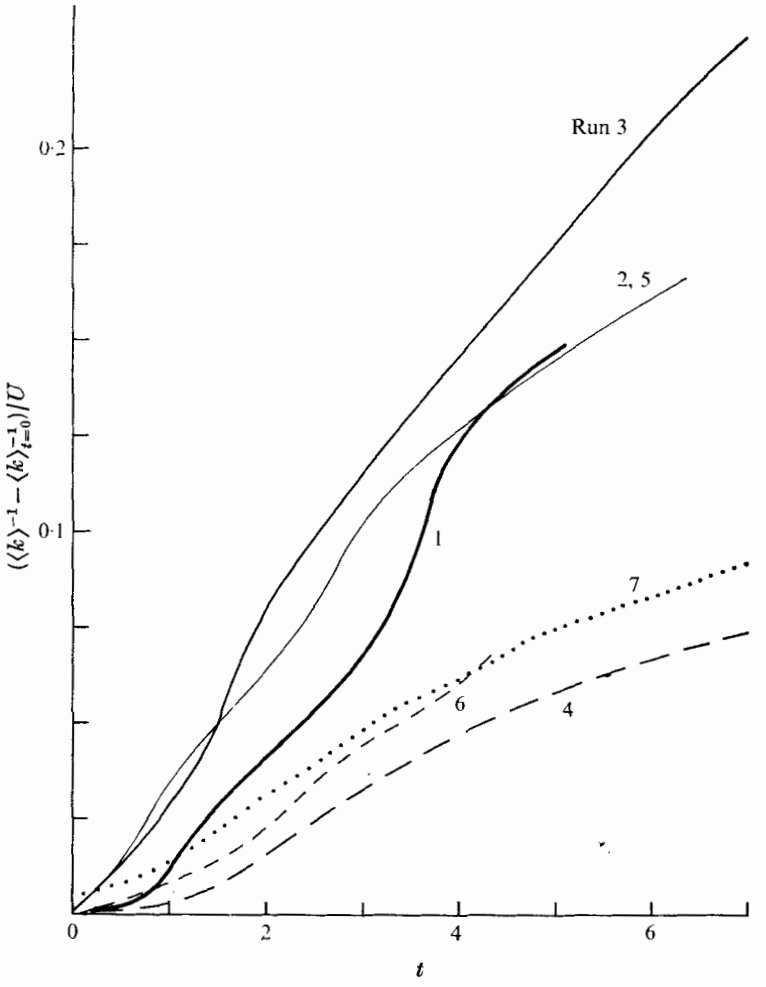

FIGURE 3. Experimental growth of the dominant scale of the eddy field with time. ——, $\beta = 0$; – – –, ·····, $\beta > 0$. U_0 is the particle velocity at time $t = 0$. Run numbers indicated.

a 'droplet' instability occurs (particularly in FD64) in which the filaments break up, artificially accelerating the cascade.

An experimental test of (2.4), figure 3 (solid curves), shows the increase with time of the dominant scale $\langle k\rangle^{-1}$ for each of the numerical models. The ordinate has been normalized by the initial r.m.s. velocity. A combination of statistical fluctuations (initial conditions were not identical) and inherent differences in accuracy caused the curves to differ. But, on the whole, the increase of scale with time occurred smoothly across $2\frac{1}{2}$ octaves of $\langle k\rangle$, with little change in rate once the spectrum had broadened and forgotten its initial form. There was some sign of the cascade slowing down when the confines of the computational box were felt (see run 2, final $\langle k\rangle = 3{\cdot}2$, or run 1, final $\langle k\rangle = 2{\cdot}2$), but perhaps less so than would be expected from Kraichnan's (1971) prediction that the cascade involves essentially wavenumbers far smaller than (say less than 20 % of) $\langle k\rangle$.

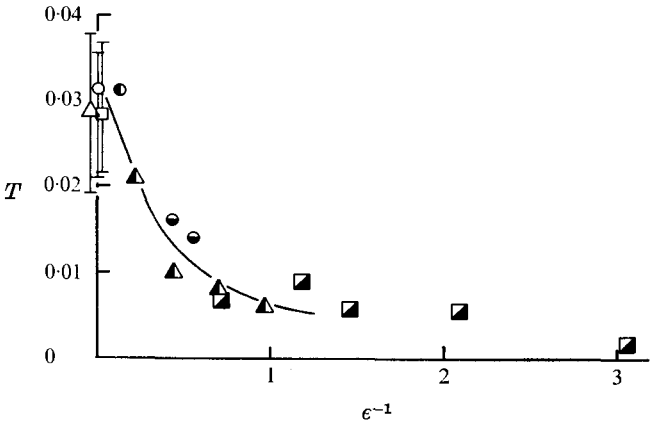

FIGURE 4. Cascade rate T *vs.* inverse wave steepness $\epsilon^{-1} = \beta/(2U\langle k\rangle^2)$. Error bars, for the pure-turbulence runs, indicate the spread of T remaining after averaging over 100 time steps. SP128: ○, run 2; ◐, run 5; ◒, run 6. SP64: □, run 3; ◪, run 7. FD64: △, run 1; ◭, run 4. Correction has been made for viscosity (T_ν). Curve faired by eye.

The cascade rate was evaluated in two ways, both from its definition

$$T = 2\int_0^\infty kF(k)\,dk/U^3\langle k\rangle$$

in terms of the transfer spectrum and by measuring the change in the mean wavenumber with time and subtracting the purely viscous contribution to the change, which is

$$T_\nu(t) = \frac{2}{R_e}\left[\frac{\langle k^3\rangle}{\langle k\rangle^3} - \frac{\langle k^2\rangle}{\langle k\rangle^2}\right],$$

where $R_e = U/\langle k\rangle\nu$ and $\langle k^n\rangle = \int k^n E\,dk/\int E\,dk$, depending on the first three moments of $E(k)$. The results were in agreement, and henceforth, and in table 1, the second method, in which $T = T_{\rm obs} - T_\nu$, is used. $T_{\rm obs}$ is just the slope of the curves in figure 3, which is shown corrected in figure 4. The purely turbulent cases ($\beta = 0$) lie along the vertical axis; the mean of each run is plotted, with brackets indicating the maximum and minimum T found in any block of 100 time steps. The value $T = 3{\cdot}00 \times 10^{-2}$ is most representative of these experiments, the standard deviation from this value being about 15%. While we cannot fully represent the physics of infinite Reynolds number, unless the truly inviscid spectra turn out to have shapes very unlike ours the corresponding T's will be similar. Other measures of the cascade could have been defined, for example $T'' \equiv \int_t |dE(k)/dt|/U^3\langle k\rangle$. In these experiments $T''/T \approx 2$.

SP128, run 2, seemed to be running at an optimal Reynolds number ($\simeq 150$), judging by figure 2, while in SP64, run 7, R_e ($\simeq 30$) was smaller than necessary, and in FD64, run 1 ($R_e \simeq 200$), it was somewhat larger than was strictly valid. Nevertheless the corrected cascade rates agree surprisingly well.

An interesting statistic describing the breadth of the wavenumber spectra is the ratio of the standard deviation about the mean to the mean:

$$\langle(k - \langle k\rangle)^2\rangle/\langle k\rangle^2 = \langle k^2\rangle/\langle k\rangle^2 - 1.$$

The initial behaviour of a narrow spectrum causes the breadth to increase. Values (table 1) for $\beta = 0$, averaged over entire runs (but omitting the period of initial transience), are 0·34 for SP128, which is the most reliable value, 0·28 for SP64 (rather viscous) and 0·68 for FD64 (rather aliased). For comparison, a model spectrum $E = k^{-4}$ for wavenumbers above some cut-off (and $E = 0$ below) gives a constant value of $\frac{1}{3}$. A k^{-3} spectrum above a cut-off is, by our definition, infinitely broad (logarithmic divergence). The breadth implied in Batchelor's solution is

$$\int_0^\infty \xi^2 f\, d\xi \Big/ \left(\int_0^\infty \xi f\, d\xi\right)^2 - 1,$$

also a constant.

The spectral shapes at large wavenumber (yet below the viscous cut-off) are quite well defined (table 1). In SP128, run 2, $E \propto k^{-4\cdot3}$, suggesting that spectra at large R_e may indeed be steeper than the famous k^{-3} law.

Waves and turbulence

The effect of wave propagation is most easily seen in time–longitude diagrams of the stream function at a single latitude, with and without β. Figures 5 (*a*) and (*b*) show a purely turbulent case, run 2 (at two latitudes, $y = 0$ and $y = \pi$). The coalescence of the initially small eddies occurs until the size of the box is approached (in these plots the apparent wavelength is somewhat greater than $2\pi/\langle k\rangle$, essentially because ψ is a smoother quantity than the velocity; the spectrum of ψ is $k^{-2}E(k)$). Beside the space–time plots are drawn triangles whose hypotenuses have slope U^{-1}. Similarity suggests that typical slopes of the contours vary with U, with constant of proportionality $2\pi T \simeq 0{\cdot}2$.

A very weak beta-effect is present in figures 5 (*c*) and (*d*), run 5, for which initial conditions were identical to those in figures 5 (*a*) and (*b*). The wave steepness ϵ was 158 at the start, so that turbulent effects dominated. By mid-run, Fourier components of larger scale began to propagate westward with phase speed given by the slopes of the ψ contours. Then ϵ had reached 15. No alteration of the purely turbulent cascade rates occurred, for the energetically dominant wavenumbers had not begun to propagate. Finally, at the end of the run, the wave steepness had reached 5·9, and westward propagation was becoming established at all latitudes (the steepness of Fourier components with $k = 2$, which contribute heavily to the figure, had descended to 2·2). The corresponding time–*latitude* plots show no systematic phase motion.

Owing to the finite computational region, which defines the largest possible eddy (hence the smallest possible ϵ), the small value of β in run 5 affected only the phase of the biggest eddies, and not the energetics; the wavenumber spectrum differed by at most a few per cent from that in run 2. Run 7 (SP64, figure 5*f*), with larger β, began roughly where run 5 left off. Westward propagation was evident at the very start, when $\epsilon = 2{\cdot}5$. It accelerated with time, as the eddies increased in size. After ϵ reached unity ($t = 2{\cdot}5$), further changes were gradual. Recalling that for simple Rossby waves the westward phase speed $c_x = \beta/k^2$ depends only on wavelength, the prediction for the transition from turbulence to waves becomes just $c_x = 2U$ (when $k = k_\beta$). For comparison, the observed c_x,

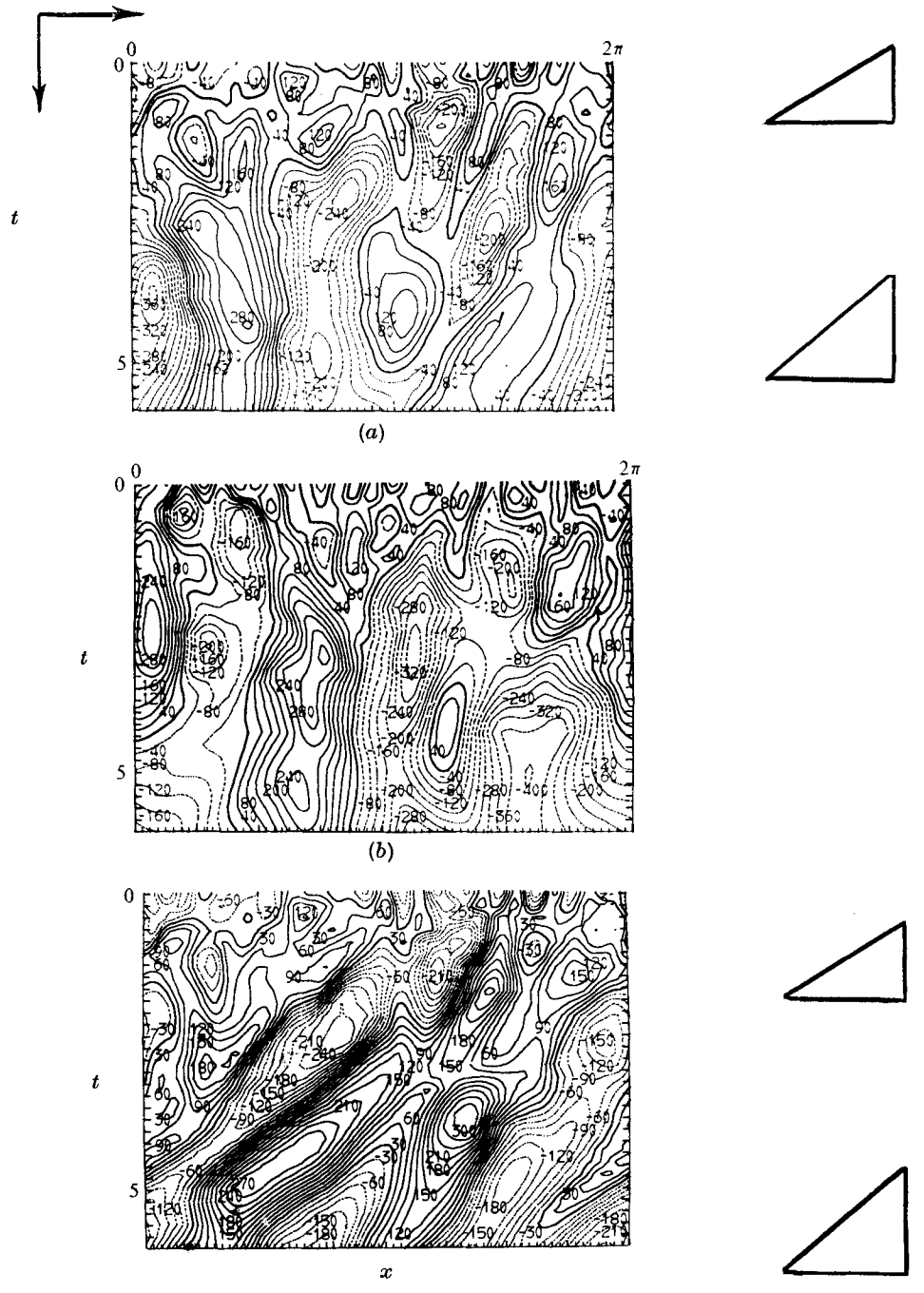

FIGURE 5. Time–longitude plot of the stream function. Time increases downwards. Triangles have hypotenuses of slope U^{-1}. Units of 10^3. (*a*) Run 2, $\beta = 0$, at latitude $y = 0$. In this purely turbulent case the scale increases without propagation. (*b*) Run 5, weak beta-effect, $\beta = 3{\cdot}25$, at latitude $y = 0$. (*c*) Run 2, $\beta = 0$, at latitude $y = \pi$. (*d*) Run 5, $\beta = 3{\cdot}25$, at latitude $y = \pi$. (*e*) Run 3, SP64, pure turbulence, $\beta = 0$, at $y = 0$. (*f*) Run 7, strong beta-effect, $\beta = 52$, at $y = 0$. Here there is some turbulent increase of scale, but westward propagation of Rossby waves dominates both the phase and, eventually, the energetics. The final quarter of the run is heavily viscous.

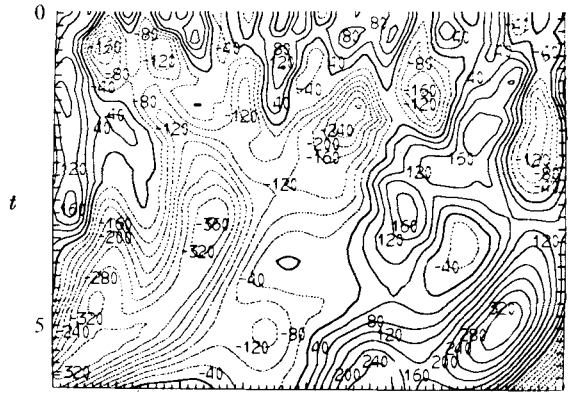

(*d*)

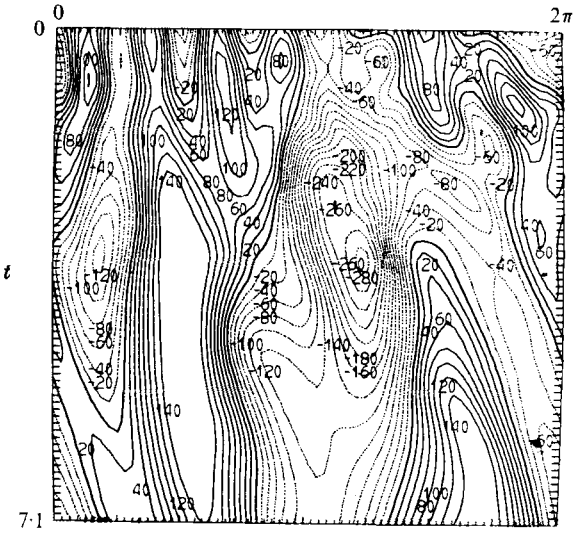

(*e*)

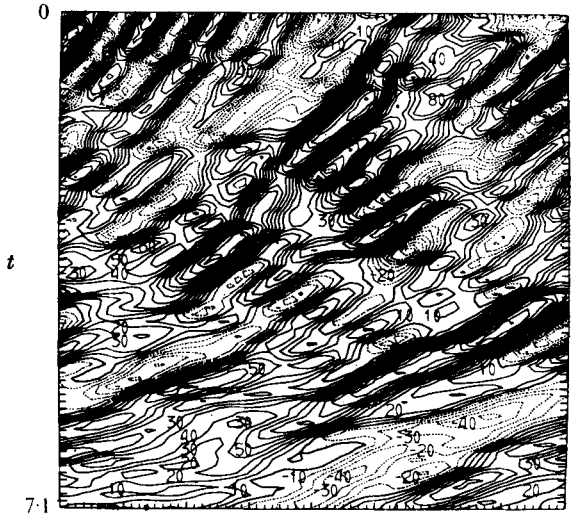

(*f*)

FIGURES 5 (*d*)–(*f*). For legend see facing page.

averaged over $3 < t < 4$, was 1·1 and $2U$ was 1·0. As these numbers and the comparison of the inclination of the phase lines with the adjacent triangles show, the field of motion seems to sense this transition by taking up the linear dispersion relation and relinquishing *nonlinear* changes in scale. Two features, however, tended to make c_x exceed $2U$ at the later stages, $t > 5$: first, components dominating the space–time plots have rather smaller wavenumber than $\langle k \rangle$, and second, the large viscosity in this run, by itself, caused $\langle k \rangle$ to decrease and ϵ to fall below unity. For comparison, figure 5 (*e*) shows the evolution from identical initial conditions but with $\beta = 0$ (run 3). Further experiments, with FD64, are reported in Rhines (1973).

The variation of the dominant scale with time is shown, for runs with the beta-effect, by dashed curves in figure 3. Despite the range of R_e present, the slowing down of the turbulent cascade is evident, particularly when pairs of runs using the same program and the same initial conditions are examined (runs 1 and 4 or 3 and 7). Figure 4, showing the cascade rate as a function of ϵ^{-1}, gives the clearest demonstration. T decreases by a factor of five between $\epsilon^{-1} = 0$ (where $T = 3 \times 10^{-2}$) and $\epsilon^{-1} = 1$ ($T = 6 \times 10^{-3}$). There is rather little scatter about the faired curve considering the variety of codes, initial conditions and Reynolds numbers, and also the inherent unpredictability of nonlinear flows.

The few points in $\epsilon^{-1} > 1$, which have entered by losing their steepness to viscosity, show values of T descending to 0·0015 at $\epsilon^{-1} = 3$. But the corrections T_ν are so large then (table 1) that we do not have great confidence in such points. Primitive integration of the equations becomes difficult in $\epsilon^{-1} \gg 1$ (if one waits for significant nonlinear effects to occur) and in this sense the computer and theoretician complement one another. Further work to better establish $T(\epsilon)$ is awaited. Kenyon's and Gill's linear theories suggest values of T of the order of those observed at both extremes: $T \lesssim 4 \times 10^{-3}$ (Kenyon, $\epsilon \ll 1$); $T \approx 3$–6×10^{-3} (Gill, $\epsilon \ll 1$); and $T \approx 1$–3×10^{-2} (Gill, $\epsilon \gg 1$).

The linear dispersion relation for Rossby waves appears to have escaped nonlinear modification for Fourier components whose ϵ was as great as 2. Table 1 shows that the experimental westward phase speed in this range, inferred from the x, t plots, usually differs from $\beta/\langle k \rangle^2$ by less than the error in determining the appropriate choice for k.

Anisotropy

Our theoretical arguments, and Kenyon's tendency calculation, predicting a growing anisotropy due to beta, were borne out in all runs. Figure 6, for example, shows the streamlines for runs 3 and 7 (SP64) at $t = 5{\cdot}1$. The eddies in run 7 manage to cluster together along latitude lines more easily than across them, and eventually form alternating bands of mean current across the fluid. The ratio of r.m.s. northward to r.m.s. westward velocity is about 0·5 and decreasing. Further examination of the prediction that the end-state of the cascade is a steady pattern of zonal jets is merited.

Vorticity and breadth

The slowing down of the energy cascade affects also the vorticity field, for it is the very movement of energy to small wavenumbers that permits squared vorticity to go to large wavenumbers. By inhibiting the former, we have removed

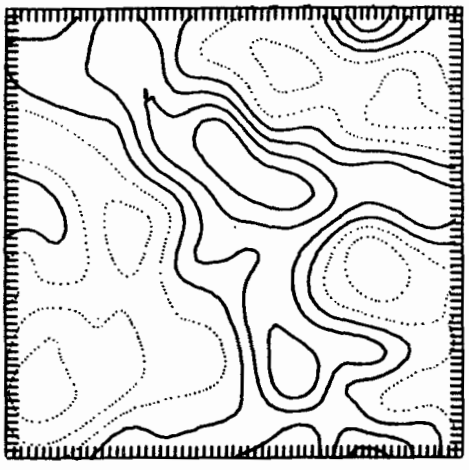

(*a*)

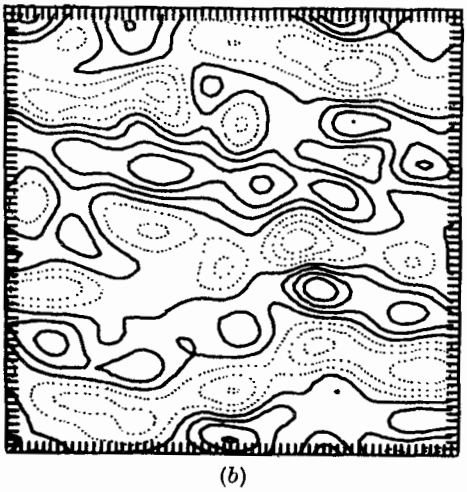

(*b*)

FIGURE 6. Streamlines at $t = 5{\cdot}1$. (*a*) Run 3, $\beta = 0$, contour interval = 0·16. (*b*) Run 7, strong beta-effect, $\beta = 52$, contour interval = 0·06. Beside keeping the scale small, beta acts to produce predominantly zonal flows.

the supply of vorticity for the latter. Given a persistent dissipation of enstrophy at large wavenumbers, the vorticity field must lose much of the fine-structure associated with two-dimensional turbulence. The shearing of the vorticity contours into thin laminae gives way to the propagation of vorticity without significant changes of wavenumber.

The energy spectra respond by narrowing. A typical value (table 1) for the evolved spectra, of the breadth, is 0·1 (with β) compared with 0·34 (without) and a typical shape of the spectrum above k_β is $k^{-5{\cdot}4}$ (with β) compared with $k^{-4{\cdot}3}$ (without). This makes ever more valid the simplified description of the field by single length, time and velocity scales (or perhaps pairs of scales, owing to the growing anisotropy), and suggests the reason for the success of the scale analysis used to establish these phenomena.

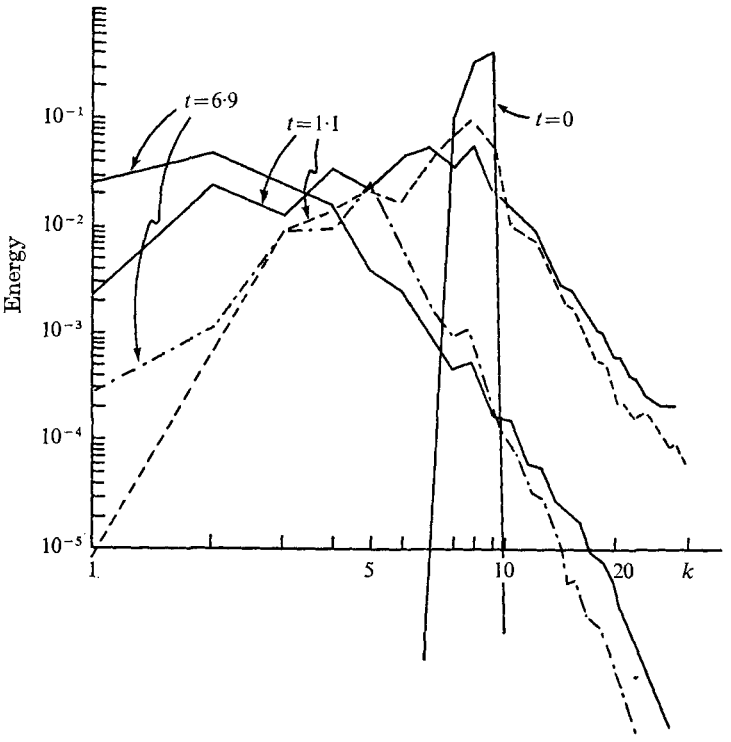

FIGURE 7. Evolution of wavenumber spectra, runs 3 ($\beta = 0$) and 7 ($\beta = 52$), from identical initial conditions. The Reynolds number is rather small, causing the tail to slope very steeply. Solid curves correspond to $\beta = 0$.

Figure 7 is a time sequence of energy spectra, with and without β, from SP64 (runs 3 and 7), corresponding to the fields shown in figure 6. In the absence of β the flow expanded quickly. The interactions† seemed to have a great reach, sending energy from a wavenumber of 10 to a wavenumber of 1 almost at the outset. With β present, the spectra evolved in smaller steps, remaining narrow and increasing the dominant scale slowly. The Reynolds number of these runs was rather small (20–40), and consequently the large wavenumber tail was steeper than normal (table 1). Other spectral plots may be found in Rhines (1973).

4. Geophysical applications and conclusion

Two-dimensional turbulence models have been applied to the dynamics of the *atmosphere*, mostly to rationalize the steep spectral slope found at large wavenumber. But it may be that such barotropic models are, instead, more relevant to (global) wavenumbers smaller than about 7, at which wavenumber kinetic

† Nonlinear barotropic models have been criticized for omitting interactions with baroclinic modes (whereas in linear constant-depth models the modes are independent), but work in preparation with a baroclinic computer model shows the present results to have extensive validity. In addition, initially pure barotropic motions remain so, even in a baroclinic model. See also Gavrilin, Mirabel & Monin (1972).

energy is being supplied from the large-scale temperature field. In this case there is need to explain the lack of violently 'red' spectra, for turbulence left to itself would quickly produce eddies of global extent. Observed spectra, however, tend to be level or to decrease at wavenumbers less than 5 (e.g. Leith 1972, figure 1).

Any of several geophysical effects neglected in the pure-turbulence model may account for this: mean-flow interactions (although the direct flux of energy from eddies to the mean flow is small, relative to other sources and sinks, the eddy field is delimited by the mean zonal flow, meanders of the jet stream in fact being a part of the nominal eddy field); dissipation by friction [Lilly (1972) recognized the short (3- to 6-day) e-folding time for kinetic energy to dissipate, and constructed a turbulence model with forcing balanced in the mean by surface drag. Energy put in, say at a wavenumber of 8, proceeds towards larger scales but is quickly damped, leading to a realistic spectrum. Use of such estimates of overall dissipation, however, may exaggerate its effect on the 'red' cascade, for less than half the observed dissipation occurs in the surface boundary layer, and the rest appears to be intermittent in space, as Lilly points out]; or, in the present case, β.

As evidence for the importance of β, the zonal wavenumber corresponding to k_β falls between 3 ($U = 15\,\mathrm{m\,s^{-1}}$, 45° latitude) and 5 ($U = 10\,\mathrm{m\,s^{-1}}$, 35° latitude), implying a barrier to the cascade, which helps to explain the observed flattening of the spectra. Indeed, Elliasen & Machenauer (1965), and of course Rossby, have invoked wave dynamics to explain the progression of phase at long and ultra-long atmospheric scales. There is also anisotropy in the observed fields reminiscent of the present experiments. Spectra of north–south winds overlie spectra of east–west winds at larger wavenumbers, but, below $k = 5$ or so, there is considerably more energy in the east–west winds (see Kao & Wendell 1970; Elliasen 1958; Baer 1972, who uses an isotropic index, so that his spectra are more like those in this paper).

Examination of the general circulation models should reveal the relative importance of wave propagation in determining the true spectrum. I hope, at least, that the present work will help in understanding the partial models of atmospheric processes. For instance, the strong dependence of T on ϵ argues against total acceptance of either Kenyon's (1967) weakly interacting model of energy near a wavenumber of 5 (which predicts too slow a cascade) or the application of pure two-dimensional turbulence at longer scales (which cascades too quickly).

For the *ocean* the transition scale k_β^{-1} is 70 km, based on $5\,\mathrm{cm\,s^{-1}}$ (barotropic component) currents at 30° latitude. (The box represents 2300 km of ocean, with the time unit 83 days.) The implied diameter of eddies is about 220 km, close to present observations. Like the atmosphere, the ocean has a wavenumber spectrum which is level or decreasing at wavenumbers smaller than k_β, as this paper would predict. The source of the 'Swallow' eddies (Crease 1962) is a subject of current interest: some candidates are baroclinic instability, either of the broad ocean circulation or of the intense boundary currents, yielding energy at scales ~ 40 km, flow over rough topography, or direct wind generation (with enhancement at the western boundary).

A word must be said about the last two effects, which were omitted from this

study. First, roughness of the sea-bed occurs at all scales. Even in the linear problem (infinitesimal currents) there is a quasi-turbulent cascade of energy from large to small scales (see Rhines & Bretherton 1973). This reversal of the 'red' cascade is allowed by a generation term in the enstrophy equation (2.5). Scale analysis and computer experiments with the linear wave problem suggest that, for topography occupying a narrow band of wavenumbers near k_h, this cascade occurs at a rate $f\delta_1$, where δ_1^2 is the variance of the depth. Comparing with two-dimensional turbulence, $Uk_h/f\delta_1$ appears as the relative measure of turbulent effects, which would lead to clustering of the eddies, and topographic effects, which would fragment them. If, instead, the bottom slopes are broader than the initially imposed eddies, they will simply act to reinforce the β-effect (f/h contours replace latitude lines), and hence to reduce the scale at which turbulence turns into waves to $(2U/h|\nabla(f/h)|)^{\frac{1}{2}}$. (Over the continental rise, for instance, depth contours act like latitude lines, and the anisotropy we predict will favour motion along these contours. It appears that, despite the stronger restoring force, eddies there are no more linear than elsewhere (Schmitz 1974).)

Second, coastal boundaries alter the problem, also by adding a generating term to the enstrophy equation. With ψ vanishing on $\mathscr{C}$, (2.7) becomes

$$\partial_t \iint_S |\nabla^2\psi|^2\,dx\,dy = -\tfrac{1}{2}\beta \oint_{\mathscr{C}} |\mathbf{u}|^2 \sin\theta_b\,ds,$$

where θ_b is the angle of a positively directed vector tangent to the boundary, with respect to east. The total enstrophy in a basin is thus not invariant, shoreline lying to the west of the fluid acting as a source and shoreline to the east as a sink. This formula applies to the nonlinear equations, whether steady or not, and affects the tendency for western intensification. (i) In a linear frictional 'Gulf Stream', for example, enstrophy produced at the western wall is dissipated by bottom friction (the generation of enstrophy by wind stress being relatively negligible); (ii) in the nonlinear frictionless free boundary currents of Fofonoff (1954), east–west symmetry allows a steady solution with enstrophy produced in the west being lost at the eastern wall; and (iii) the linear reflexion of Rossby waves (Phillips 1966; Pedlosky 1965) at the western wall converts large-scale energy to small-scale energy, increasing the total enstrophy. Combined with the notion that small-scale (large enstrophy/energy) motions propagate slowly, the integral relations give general cause for the concentration of both energy and enstrophy to the west. The presence of energetic, small eddies in the Sargasso Sea may in part verify this effect, but the other sources are also working nearby. Distinction between boundary-induced eddies and eddies of the sort we have considered here may be possible by observing their orientation: the former should have predominantly north–south currents, while the latter should favour east–west currents (or those along f/h contours).

There may be applications of these turbulent models other than to energetic questions. The study of lateral mixing of water masses depends on the understanding of the same advection working in figure 2(*a*). Observations in the North Atlantic of the shapes of sheared patches of Mediterranean water and of intrusions at the Gulf Stream front are examples.

Turbulence in this study acts as a source of waves. In three dimensions, waves seem more often to feed turbulence, the reverse process occurring only at a low efficiency (see Rhines 1973). Here, in addition, the restoring forces contrive to sharpen the energy spectra while dispersing energy in physical space. The distinction between turbulent and wavelike dynamics corresponds simply to the frequency of occurrence of closed contours in maps of the potential vorticity $\nabla^2\psi + \beta y$. Only at energy levels small enough that the contours are predominantly open, and the northward gradient of potential vorticity is persistently felt, can organized propagation occur. As run 5 showed, however, phase propagation obeying the linear dispersion relation may be embedded in energetics which are rather nonlinear.

The author is grateful to the National Science Foundation for support (GX-36342), and to the National Center for Atmospheric Research for providing the extensive computing time (NCAR is supported by the National Science Foundation). This is contribution no. 39 of the Mid-ocean dynamics experiment and contribution no. 3316 of the Woods Hole Oceanographic Institution. Dr Fox, Dr Lilly and Dr Orszag generously provided major parts of the computational codes.

Appendix. Note on inertial ranges

We have considered here the transient behaviour of the energy-containing eddies, which is predictable independently of inertial-range arguments. The recent literature, however, has centred on the possibility that inertial ranges, in equilibrium and local in wavenumber, may exist. The enstrophy inertial range may be compatible with Batchelor's transient solution, for which the energy flux F is $-Ek/t$ and enstrophy flux G is

$$-t^{-1}k^3E + 2t^{-1}\int_0^k k^2E\,dk,$$

if F, $G_k \to 0$ sufficiently closely in such a range. But Kraichnan (1971) has shown that such a range is far less local than energy-carrying ranges in either two or three dimensions. His spectrum $E \propto k^{-3}(\ln(k/k_1))^{-\frac{1}{3}}$ is sensitive to the position of the energetic peak, near k_1, and any steeper choice of the spectrum (such as those occurring in our experiments) will be dominated by energy near k_1: all components of the flow then reflect the nature of the big eddies (in accord with the simplified description of the field by single scales L, τ and U).

The impetus to establish the enstrophy range seems to have come through analogy with energy flow in three-dimensional turbulence. But, in addition to the lesser importance of enstrophy, the analogy obscures the *slowness* of the enstrophy cascade: as $\nu \to 0$ it takes an infinite time for enstrophy to reach dissipation wavenumbers (the time required to flow from a wavenumber k_1 to $k \gg k_1$ is $\gtrsim \left(\int_0^\infty k^2E\,dk\right)^{-\frac{1}{2}} \ln(k/k_1)$). This is in contrast with the efficiency of three-dimensional turbulence, where at large Reynolds number the energy is

dissipated rapidly, in a time $\sim (k_1 U)^{-1}$. The arguments about the nature of the inviscid limit are thus far less important in two dimensions, for enstrophy dissipation vanishes for all finite times if $\nu = 0$. The upward enstrophy flux

$$G_\infty = 2t^{-1}\int_0^\infty k^2 E\, dk$$

as $k \to \infty$ in Batchelor's transient solution does not imply the contrary, only that the solution fails to be uniformly valid for any finite time.

REFERENCES

BAER, F. 1972 An alternate scale representation of atmospheric energy spectra. *J. Atmos. Sci.* **29**, 649.

BATCHELOR, G. K. 1953 *Homogeneous Turbulence.* Cambridge University Press.

BATCHELOR, G. K. 1969 Computation of the energy spectrum in homogeneous two-dimensional turbulence. *Phys. Fluids Suppl.* **12**, II 233.

CREASE, J. 1962 Velocity measurements in the deep water of the western north Atlantic. *J. Geophys. Res.* **68**, 3173.

ELLIASEN, E. 1958 A study of long atmospheric waves on the basis of zonal harmonic analysis. *Tellus*, **10**, 206.

ELLIASEN, E. & MACHENAUER, R. 1965 A study of the fluctuations of the atmospheric flow patterns. *Tellus*, **17**, 220.

FOFONOFF, N. P. 1954 Steady flow in a frictionless, homogeneous ocean. *J. Mar. Res.* **13**, 257.

FOX, D. G. & ORSZAG, S. A. 1972 Inviscid dynamics of two-dimensional turbulence. *Nat. Center Atmos. Res. MS.* no. 72-80.

GAVRLIN, B. L., MIRABEL, A. P. & MONIN, A. S. 1972 On the energy spectrum of synoptic processes. *Isv. Atmos. Ocean. Phys.* **5**, 483 (in Russian).

GILL, A. E. 1974 The stability of planetary waves on an infinite beta-plane. *Geophys. Fluid Dyn.* **5**, 29–47.

HASSELMANN, K. 1967 A criterion for nonlinear wave stability. *J. Fluid Mech.* **30**, 737.

HERRING, J. R., ORSZAG, S. A., KRAICHNAN, R. H. & FOX, D. G. 1974 Decay of two-dimensional homogeneous turbulence. *J. Fluid Mech.* **66**, 417.

KAO, S. K. & WENDELL, L. 1970 The kinetic energy of the large-scale atmospheric motion in wavenumber–frequency space. *J. Atmos. Sci.* **27**, 359.

KENYON, K. 1964 Nonlinear energy transfer in a Rossby-wave spectrum. *Geophys. Fluid Dynamics Program, Woods Hole, Massachusetts.*

KENYON, K. 1967 Discussion. *Proc. Roy. Soc.* A **299**, 141.

KRAICHNAN, R. H. 1967 Inertial ranges in two-dimensional turbulence. *Phys. Fluids*, **10**, 1417.

KRAICHNAN, R. H. 1971 Inertial-range transfer in two- and three-dimensional turbulence. *J. Fluid Mech.* **47**, 525.

LEITH, C. E. 1972 Atmospheric predictability and two-dimensional turbulence. *J. Atmos. Sci.* **28**, 145.

LILLY, D. K. 1969 Numerical simulation of two-dimensional turbulence. High-speed computing in fluid dynamics. *Phys. Fluids Suppl.* **12**, II 240.

LILLY, D. K. 1971 Numerical simulation of developing and decaying two-dimensional turbulence. *J. Fluid Mech.* **45**, 395.

LILLY, D. K. 1972 Numerical simulation studies of two-dimensional turbulence. I. *Geophys. Fluid Dyn.* **3**, 289.

LONGUET-HIGGINS, M. S. & GILL, A. E. 1967 Resonant interactions between planetary waves. *Proc. Roy. Soc.* A **299**, 120.

LORENZ, E. N. 1972 Barotropic instability of Rossby wave motion. *J. Atmos. Sci.* **29**, 258.

MCEWAN, A. D. 1972 Resonant degeneration of resonantly-excited standing internal gravity waves. *J. Fluid Mech.* **50**, 431.

MARTIN, S., SIMMONS, W. & WUNSCH, C. 1972 The excitation of resonant triads by single internal waves. *J. Fluid Mech.* **53**, 17.

NEWELL, A. C. 1970 Rossby wave packet interactions. *J. Fluid Mech.* **35**, 255.

ONSAGER, L. 1949 Statistical hydrodynamics. *Nuovo Cimento*, **6**, 279.

ORSZAG, S. A. 1971 Numerical simulation of incompressible flows with simple boundaries: accuracy. *J. Fluid Mech.* **49**, 75.

PEDLOSKY, J. 1965 A note on the western intensification of the oceanic circulation. *J. Mar. Res.* **23**, 207.

PHILLIPS, N. A. 1966 Large-scale eddy motion in the western Atlantic. *J. Geophys. Res.* **71**, 3883.

PHILLIPS, O. M. 1966 *The Dynamics of the Upper Ocean*, p. 109. Cambridge University Press.

RHINES, P. B. 1973 Observations of the energy-containing oceanic eddies, and theoretical models of waves and turbulence. *Boundary Layer Met.* **4**, 345.

RHINES, P. B. & BRETHERTON, F. B. 1973 Topographic Rossby waves in a rough-bottomed ocean. *J. Fluid Mech.* **61**, 583.

SCHMITZ, W. J. 1974 Observations of low-frequency current fluctuations on the continental slope and rise near Site D. *J. Mar. Res.* **32**, 233.

SIMMONS, W. F. 1969 A variational method for weak resonant wave interactions. *Proc. Roy. Soc.* A **309**, 551.

STARR, V. P. 1968 *Physics of Negative Viscosity Phenomena*. McGraw-Hill.

TAYLOR, G. I. 1917 Observations and speculations on the nature of turbulent motion. *Scientific Papers*, vol. 2 (ed. G. K. Batchelor), p. 69. Cambridge University Press.